International Journal of Engineering Science Invention (IJESI)
ISSN (Online): 2319 – 6734, ISSN (Print): 2319 – 6726
www.ijesi.org ||Volume 7 Issue 5 Ver VI || May 2018 || PP 07-17

Spectral Investigations and Emission Properties Of Ho^{3+} Doped Different Phosphate Glasses For 2µm Laser Materials

B. Haritha*, S. Damodariah, V. Reddy Prasad, Y.C. Ratnakaram
Department of Physics, S. V. University, Tirupati-517 502, A.P, India
Corresponding auther : B. Haritha

Abstract : *Ho^{3+} doped different phosphate glasses with chemical compositions 69.5$NH_4H_2PO_4$ -15 Na_2CO_3-15MCO_3) (M=Li, Mg, Ca and Ba) were prepared using melt quenching method. For these glasses, structural and spectroscopic properties were characterized through X-ray diffraction, optical absorption, photoluminescence and solid state ^{31}P NMR techniques. From the absorption spectra, spectral intensities (f_{exp} and f_{cal}), Judd-Ofelt intensity parameters (Ω_2, Ω_4, Ω_6), total radiative transition probabilities (A_T), radiative lifetimes (τ_R) and branching ratios (β_R) were obtained for all Ho^{3+} doped phosphate glass matrices. From the photoluminescence spectra, peak stimulated emission cross-sections (σ_e) were calculated for different Ho^{3+} doped phosphate glasses. The Ho^{3+} doped phosphate glasses show strong green emission at 545 nm and red emission at 656 nm under excitation at 450 nm. The measured lifetimes (τ_{meas}) of the excited $^5F_5$ state, of Ho^{3+} were obtained from decay profiles. From this analysis, it is concluded that Ho^{3+} doped Li phosphate glass exhibit relatively better properties for the application in mid infrared laser at a wavelength of 2.0 µm.*

Date of Submission: 10-05-2018 Date of acceptance: 28-05-2018

I. INTRODUCTION

Glasses doped with rare earth metal ions have several advantages and applications for solid state lasers operating in the visible to Infrared (IR) spectral ranges. These materials have various applications in optical amplifiers, waveguides, optical data storages, sensors, optical displays and optical devices [1-6]. The main advantage of these glasses is that they can be fabricated very easily with large homogenous pieces having non-linear refractive indices. Among various oxide glasses, phosphate glasses have several prominent features over conventional silicate glasses such as high transparency, low melting point, low refractive index, low dispersion and high ultra violet transmission [7]. These properties of phosphate glasses make them attractive materials for device fabrication. Spectroscopic properties of rare earths doped crystals or glass hosts were mainly used because of their efficient lasing action in many of them. Among various rare-earth ions, Ho^{3+} ion is known to exhibit intense luminescence in the green, red and NIR regions in the glass hosts [8, 9]. Hence such amorphous materials are highly useful in traffic signals. Optical properties of Ho^{3+} ion doped glass systems have been investigated and reported luminescent properties in both from down conversion as well as up conversion which covers visible, near infrared and mid infrared regions [10-12].

Ho^{3+} ion has several advantages than the other rare earth metal ions. In its trivalent state, it has large number of energy levels and radiative transitions. Ho^{3+} ion can be sensitized by a variety of lanthanide ions or transition metal ions to achieve efficient laser emission [13]. Ho^{3+} ion has high emission cross-section, broad emission band and long fluorescent lifetime which makes Ho^{3+} ion more suitable for generating 2µm laser radiation due to $^5I_7 \rightarrow {}^5I_8$ transition. These 2 µm lasers have various applications in the high resolution spectroscopy of low pressure gases, laser medicine surgery, eye safe lasers, atmospheric pollution monitoring, military, laser distance measurement and so on [14-15].

Recently, Kesavalu et. al [16] investigated optical spectroscopy and emission properties of Ho^{3+} doped gadolinium calcium silicoborate glasses for visible luminescence devices applications. Rong Chen et.al [17] reported 2 µm fluorescence of Ho^{3+}: $^5I_7 \rightarrow {}^5I_8$ transition sensitized by Er^{3+} in tellurite germinate glasses. Srinivasa Rao et.al [18] studied optical properties of Ho^{3+} ions in lead phosphate glasses. Ravi Kumar et.al [19] studied influence of red lead on the intensity of green and orange emission of Sm^{3+} and Ho^{3+} co-doped ZnO-SrO-P_2O_5 glass system. Ying et.al [20] studied 2µm emission of Ho^{3+} doped fluoro phosphate glass sensitized by Yb^{3+}.

In the present work, vibrational and structural modes in the phosphate glass units were investigated using solid state NMR studies and are reported. Various spectroscopic parameters like electric dipole linestrengths (S_{ed}), radiative transition probabilities (A_T), radiative lifetimes (τ_R) and integrated absorption coefficients ($\sum$) are calculated from the absorption spectra of Ho^{3+} doped different (Li, Ba, Mg and Ca) phosphate glasses using Judd-Ofelt theory. The laser characteristic parameters such as branching ratios (β) and stimulated emission cross-sections (σ_p) are obtained from the emission spectra of Ho^{3+} doped different

phosphate glass matrices and are compared with the parameters in other materials. From these studies, few transition in phosphate glass matrix.

II. Experimental

2.1 Material synthesis

In this study, the authors prepared and investigated four different Ho^{3+} doped phosphate glasses using the chemicals, $NH_4H_2PO_4$, Na_2CO_3, Li_2CO_3, $BaCO_3$, $MgCO_3$, $CaCO_3$ and Ho_2O_3. The method of preparation is a melt quenching technique. All the chemicals were analar grade with 99.9% purity and were taken according to the calculated proportions of the glass composition. Final glass compositions of the prepared glass samples are marked as follows.

1. $69.5NH_4H_2PO_4$ -$15Na_2CO_3$ -$15Li_2CO_3$- $0.5Ho_2O_3$ - Li glass
2. $69.5NH_4H_2PO_4$ -$15Na_2CO_3$ -$15Ba_2CO_3$- $0.5Ho_2O_3$ - Ba glass
3. $69.5NH_4H_2PO_4$ -$15Na_2CO_3$ -$15Mg_2CO_3$- $0.5Ho_2O_3$- Mg glass
4. $69.5NH_4H_2PO_4$ -$15Na_2CO_3$ -$15Ca_2CO_3$- $0.5Ho_2O_3$ - Ca glass

The raw materials were thoroughly mixed in an agate mortar until a smooth and homogeneous mixture was obtained. Then the mixture was heated and melted in an electronic furnace at the temperature 950^0C–1000^0C for one hour in the porcelain crucible to obtain bubble free homogeneous melt. The melt was suddenly quenched by pouring it on a preheated brass plate and pressed by another brass plate. The obtained glasses were subsequently annealed at 300 ^{0}C for 2h to remove thermal strains and cracks produced inside and then allowed to cool down to room temperature. The glass samples were polished to a higher degree before measuring the optical properties.

2.2 Spectroscopic measurements

The densities were measured by Archimede's principle using water as an immersion liquid. Refractive index measurements were performed using an Abbe refractometer at sodium wavelength (584.3nm) with 1-bromonapthalene ($C_{10}H_7Br$) as a contact liquid. These refractive index values are in the range 1.525-1.551 for different Ho^{3+} doped glass matrices. The amorphous nature of the prepared phosphate glasses are confirmed through the X-ray diffraction (XRD) studies using SIEFERT diffractometer employing CuK_α radiation at 40 kV applied voltage and 30mA anode current with a Si detector. The range of diffractometer is 10^0-80^0 with step size of 0.02^0. SEM images were recorded using Caral Zeiss EVOMA15 scanning electron microscope. Solid state NMR spectra were recorded to further study the structural evolution of prepared glasses using JEOL DELTA 2 NMR at 9.4T with a 4mm probe. The acquisition time was 18ms and pulse width was 2.9µs. The optical absorption spectral measurements were done using Varian Cary 5000 spectrophotometer in UV-Vis region with 0.01 nm steps, with the resolution of <0.05 and <0.2 in the UV and Vis regions respectively. 488nm line of Ar^+ laser is used as an excitation source to record the photoluminescence spectra. The lifetime measurements were carried out using a mechanical chopper with a multi-channel scalar interfaced to a personal computer. The photoluminescence spectra and the decay curves of Ho^{3+} doped glass samples were recorded using Jobin-Yvon Fluorolog 3 spectrofluorimeter (Horiba FL3-22iHR320). All these measurements were conducted at room temperature.

III. Results and Discussion

3.1 XRD and SEM analysis

In order to study the amorphous state of prepared phosphate glasses, samples have been subjected to XRD (X-ray diffraction) analysis. It is found that all the glass samples are amorphous in nature because of the absence of sharp peaks and reflections in the XRD patterns. The XRD pattern of Ho^{3+} ion doped lithium phosphate glass is shown in Fig. 1a. From fig. 1b one can observe no bubbles or crystals or clusters in the bulk glass, which shows that the glass can be used in optical applications.

3.2 ^{31}P NMR Spectroscopy

^{31}P solid state NMR is a very important tool in characterizing structures of phosphate-type glasses due to shift in the chemical shifts being sensitive to the phosphorus environment. The phosphate bonding is analyzed through Q^n species, where the superscript n refers to the number of bridging oxygen's per tetrahedron. The solid state ^{31}P NMR spectra of different phosphate glass matrices are shown in Fig. 2. It is noticed that Li, Mg, Ca and Ba phosphate glasses are exhibiting the signals with chemical shifts –20.8, -24.7, -21.8, -22.1 ppm respectively. The observed peaks of these phosphate glass matrices are due to essentially of the Q^2 (metaphosphate) species [21]. The signal has single symmetric Q^2 peak which indicates the existence of no other Q^0 (phosphate tetrahedral with zero bridging oxygen's), Q^1 (phosphate tetrahedral with one bridging oxygen's) and Q^3 (phosphate tetrahedral with three bridging oxygens) structural units.

3.3 Fourier Transform Infrared Spectroscopy (FTIR)

The presence of functional and structural groups of prepared 0.5 mol% Ho^{3+} doped different phosphate glass matrices are analyzed in the range 400–4000 cm^{-1} using transmission spectra, which are shown in Fig. 3. Several transmission bands are observed from infrared spectrum. Results obtained from FTIR spectra regarding different vibrational bands and their assignments are given below as per given in ref. [22-23].

1. The band at 529 cm^{-1} (a) is assigned to the bending mode of O–P–O in the Q^1 units.
2. The band at 759 cm^{-1} (b) is attributed to the symmetric stretching vibration of P –O–P rings (Q^2 species).
3. The bands observed at 1258 (c) and 1636 cm-1(d) are attributed to the asymmetric stretching of (PO_2)- in the Q^2 units.
4. The bands at 2386 (e) and 2916 cm^{-1} (f) are due to the hydrogen bonding.
5. The band at 3450 cm^{-1} (g) is due to symmetric stretching vibrations of hydroxyl groups (O–H).

3.4 Absorption spectra and Judd- Ofelt theory:

The absorption spectra of Ho^{3+} doped different phosphate glasses were recorded in the wavelength region 300-700 nm and are shown in Fig.4. The bands observed are originating from the ground level $^5I_8$ to various excited levels of Ho^{3+} ion within the 4f shell. The observed absorption bands in lithium phosphate glass are appeared at 359.7, 383.6, 416.1, 448.5, 469, 484.3, 535.6 and 640 nm corresponding to transitions from the ground level $^5I_8$ to the various excited levels, $^3H_5$+$^3H_6$, $^3G_4$+$^3K_7$, $^5G_5$, $^5G_6$, $^5F_2$, $^5F_3$, $^5F_4$+$^5S_2$ and $^5F_5$, respectively. The observed absorption bands are compared based on energy bands of other reported Ho^{3+} glass systems [24]. Among various absorption bands, the band, $^5G_6$ has high intensity in the visible region centered at 22297 cm^{-1}. The optical absorption spectra are analyzed to find the experimental spectral intensities for the observed absorption bands and then Judd-Ofelt (J-O) intensity parameters (Ω_2, Ω_4, Ω_6) are calculated using the formula given in the Ref. [25]. These parameters are used to determine the local structure and bonding vicinity of Ho^{3+} ion. The experimental and calculated spectral intensities of different absorption bands of Ho^{3+} doped different phosphate glasses are obtained using the formulae given in the ref. [26-27] and are presented in Table 1. From the table, it is observed that the value of experimental (f_{exp}) and calculated (f_{cal}) spectral intensities are higher for $^5I_8 \rightarrow {}^5G_6$ transition in all the glass matrices. The accuracy of fit between the experimental and calculated spectral intensities is given by root mean square (rms) deviations. It is noticed from the table that the experimental spectral intensities are in good agreement with the calculated values for most of the transitions; the relative

According to J-O theory, the magnitudes of three phenomenological parameters known as J-O intensity parameters, Ω_λ (λ=2, 4, 6) are characterized by the intensities of absorption bands which depend on local environment. These relative magnitudes of Ω_λ parameters are useful in explaining the bonding, symmetry and stiffness of the host materials [28]. These values are presented in Table 2 along with Ho^{3+} doped different phosphate glass matrices. Among the three intensity parameters, the Ω_2 parameter reflects the intensity of the hypersensitive transition and covalence of the metal ligand bond where as Ω_4 and Ω_6 parameters indicate the rigidity of the host matrix [29]. From the magnitude of Ω_2 parameter it is observed that the covalency is in the order Li>Mg>Ca>Ba in these Ho^{3+} doped phosphate glasses. Among these four phosphate glasses Li has high degree of covalencey and Ba has low degree of covalency. In the phosphate glasses, the degree of covalency decreases with the radius of modifiers. As the radius of the modifiers increases, the distance between the rare earth ions and oxygen increases and becomes less compact in nature and low coordination with oxygen ligand.

In the present work, the trend of magnitudes of J-O intensity parameters for Li, Mg, Ca and Ba phosphate glasses is $\Omega_2>\Omega_4>\Omega_6$. Similar trend is observed in other reported glasses such as tellurite [30], Lu_2SiO_5 crystal [31], Gallium lanthanum sulphide [32] and oxyflouride (Si based) [33]. The magnitudes of Ω_4 and Ω_6 parameters depend on the viscosity and dielectric constant of the media and these parameters were also affected by the vibronic transitions of the ions bounded to the ligand atoms [34]. Ω_4 parameter is affected by the factors causing the changes of Ω_2 and Ω_6. Ω_6 parameter is higher in Mg phosphate glass matrix and lower in Ba phosphate glass matrix indicating higher and lower rigidities and viscosities respectively.

3.5 Hypersensitive transition

The intensities of certain f-f transitions are larger compared to other transitions and are characterized by the higher values of reduced matrix element $||U^2||^2$. These transitions are known as hypersensitive transitions i.e. sensitive to the inhomogeneity of ligand environment and follows the selection rules, $\Delta L \leq 2$, $\Delta J \leq 2$ and $\Delta S=0$ [35]. In the present work, only one hypersensitive transition i.e., $^5I_8 \rightarrow {}^4G_6$ of Ho^{3+} is observed. The peak positions and the intensities of this transition are very sensitive to the environment. In the present work, it is observed that the intensity of the hypersensitive transition $^5I_8 \rightarrow {}^4G_6$ decrease with the decrease of Ω_2 parameter from Li to Ba glass matrices, which is due to the strong interaction between 4f and 5d orbitals [35]. For the hypersensitive transition, the shift of the peak wavelength towards longer wavelengths indicates the increase of

degree of covalency of RE-O bond. In the present work it is observed that there is no shift of the peak wavelength of the hypersensitive transition for Li, Mg, Ca and Ba glass matrices

3.6 Radiative and non-radiative properties

Using Judd-Ofelt intensity parameters, various radiative properties like energies (Δν), electric dipole linestrengths (S_{ed}), radiative transition probabilities (A), radiative branching ratios (β_R) and integrated absorption cross sections (Σ) are calculated. These values are presented in Table 3 for lithium phosphate glass. Calculated total radiative transition probabilities (A_T) and radiative lifetimes (τ_R) for different excited states, $^3H_5$, $^5G_6$, $^3K_8$, $^5F_2$, $^5F_3$ and $^5F_4$ of Ho^{3+} doped different phosphate glasses are presented in Table 4. From the table, it is observed that the total radiative transition probability values are higher and lower for $^5G_6$ and $^3K_8$ states for all glass matrices. Among the four glass matrices, Li and Ba glass matrices have higher and lower total radiative transition probability values. Among all excitation states, $^5G_6$ and $^3K_8$ have lower and higher values of radiative lifetimes (τ_R) in all the phosphate glasses. Among all these four glasses, lower radiative lifetimes are observed in Mg glass and higher radiative lifetimes are observed in Ba glass. The exponential dependence of the multiphonon relaxation rate, W_{MPR}, on the energy gap to the next lower level ΔE, has been experimentally established for a number of crystals and glasses [36].

3.7 Luminescence properties

The excitation spectra are recorded in the spectral range 350-500nm for Ho^{3+} doped different phosphate glasses using the emission at 545 nm and are shown in Fig. 5 for different glass matrices. From the figure it is observed that spectrum consists 6 excitation bands. These observed excitation bands are centered at 361, 385, 417, 450, 474 and 486 nm corresponding to transitions from the ground state to different excited states $^3H_5$, $^5G_4$, $^5G_5$, $^5G_6$, $^5F_2$, and $^5F_3$ respectively. Fig. 6 shows the emission spectra of Ho^{3+} doped different phosphate glasses recorded using the excitation at 450 nm. In the emission spectra, three peaks are observed corresponding to the transitions, $(^5S_2)^5F_4 \rightarrow {}^5I$, $^5F_5 \rightarrow {}^5I_8$ and $(^5S_2)\,^5F_4 \rightarrow {}^5I_7$ at 545 nm, 656 nm and 752 nm, respectively. Among the three transitions, $^5F_5 \rightarrow {}^5I_8$ is more intense and very dominant in red region. In the present work, the emission peak, corresponding to the transition, $^5F_5 \rightarrow {}^5I_8$ splits into two peaks in all phosphate glasses matrices expect for Ba glass. The peak to peak separation for Li, Mg and Ca glass matrices are 694, 370 and 412 cm^{-1} respectively. The splitting was not observed in Ba glass matrix due to structural changes. It is observed that peak to peak separation is maximum in the case of Li glass and minimum in the case of Mg glass. The peak intensity ratios I_L/I_S are calculated for all glass matrices. These values are 0.313, 0.810 and 0.961 for Li, Mg and Ca phosphate glasses respectively. It is observed that intensity ratios are minimum in Li glass and maximum in Ca glass. From the emission spectra, peak positions (λ_p), effective band widths ($\Delta\nu_{eff}$), transition probabilities (A_R), stimulated emission cross-sections (σ_e) and radiative branching ratios (β_{exp}) are obtained for the observed emission transitions of Ho^{3+} doped different phosphate glasses and are presented in Table 5. Among the three transitions, the transition, $^5F_5 \rightarrow {}^5I_8$ which falls in green region is much sharper than the others which is the essential characteristic for luminescent materials. The experimental branching ratios (β_{exp}) are calculated by measuring the areas under the three emission curves. Among the three emission transitions, the transition, $^5F_5 \rightarrow {}^5I_8$ shows higher branching ratios. The branching ratio values for this transition are 0.576, 0.574, 0.584, and 0.673 for Li, Mg, Ca, and Ba phosphate glasses respectively.

The stimulated emission cross section (σ_e) is one of the important parameters used to know the material suitable for good optical material. A good optical material has large emission cross-section. The stimulated emission cross-section values are calculated for all the observed emission transitions of Ho^{3+} doped different phosphate glasses and are presented in the table 5. Among all the emission transitions of Ho^{3+} ion, σ_e values are higher for the transition, $(^5S_2)^5F_4 \rightarrow {}^5I_8$ compared to remaining emission transitions. Among all the four phosphate glasses, Li glass shows higher value of simulated emission cross-section. Glass having higher emission cross-section may be useful for good red luminescent action at the wavelength region 680 nm. Table 6 gives calculated branching ratios (β_R) and integrated absorption cross-sections (Σ) of different transitions of Ho^{3+} doped Li, Mg, Ca and Ba phosphate glass matrices. It is observed that among various transitions, $^5G_6 \rightarrow {}^5I_7$, $^3K_8 \rightarrow {}^5I_7$ and $^5F_4 \rightarrow {}^5I_7$ are having higher β_R values. The partial energy level diagram along with radiative emissions from the excited luminescent level $^5G_5$ to different lower levels is shown in Fig. 7. Under excitation of 450 nm, Ho^{3+} ions are excited to uppermost excited levels and then decays non-radiatively to the lower lying levels $(^5S_2)^5F_4$ and $^5F_4$ excited levels.

3.8 Decay rate analysis

Fluorescence decay curves of the excited level, $^5F_5$ of Ho^{3+} ion doped different phosphate glasses are obtained using the emission and excitation wavelengths, 450 and 345 nm respectively and are shown in Figure 8. From the figure, it is observed that all the decay profiles exhibit non-exponential nature. This nature is due to the presence of non-radiative channels. Measured lifetimes of the excited level, $^5F_5$ of Ho^{3+} doped different phosphate glasses are obtained from decay profiles and are presented in Table 7. The lifetime decay constants

are estimated using the formula given in Ref. [38]. From the table it is observed that the lifetime is higher for Ba glass and lower for Li phosphate glass. The measured lifetimes of $^5F_5$ of Ho^{3+} ion doped different phosphate glasses are lower than the calculated lifetimes due to the existence of non-radiative channels. The non-exponential behavior in Ho^{3+} phosphate glass matrices indicates similar local environment of holmium ion for all glass matrices. The quantum efficiencies (η) are calculated for $^5F_5$ level of Ho^{3+} in all the Ho^{3+} doped phosphate glass matrices and are presented in Table 7. From the table, it is observed that the quantum efficiency is higher (80 %) for Li phosphate glass matrix. Hence, Li glass of Ho^{3+} ion are selected for lasing transition in phosphate glass matrix.

Figure captions:

Fig. 1 (a) XRD profiles and (b) SEM image of 0.5 Mol % Ho^{3+} doped different phosphate glasses.
Fig. 2 ^{31}P Solid state NMR Spectra of Ho^{3+} doped different phosphate glasses.
Fig. 3 FT-IR spectra of Ho^{3+} doped different phosphate glasses
Fig. 4 Optical absorption spectra of Ho^{3+} doped different phosphate glasses.
Fig. 5 Excitation spectra of Ho^{3+} doped different phosphate glasses
Fig. 6 Emission spectra of Ho^{3+} doped different phosphate glasses.
Fig. 7 Partial energy level diagram for Ho^{3+} doped lithium phosphate glass.
Fig. 8 Decay profiles of Ho^{3+} doped different phosphate glasses.

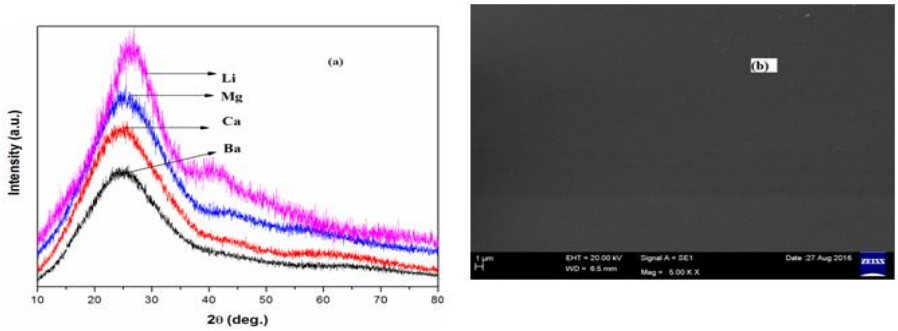

Fig. 1

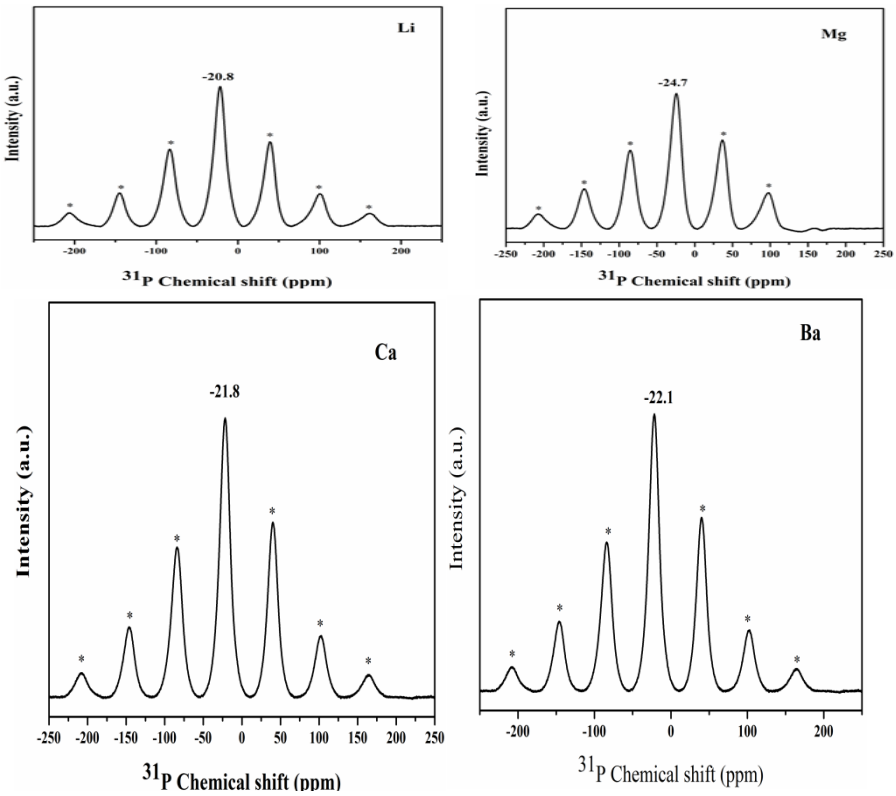

FIG.2

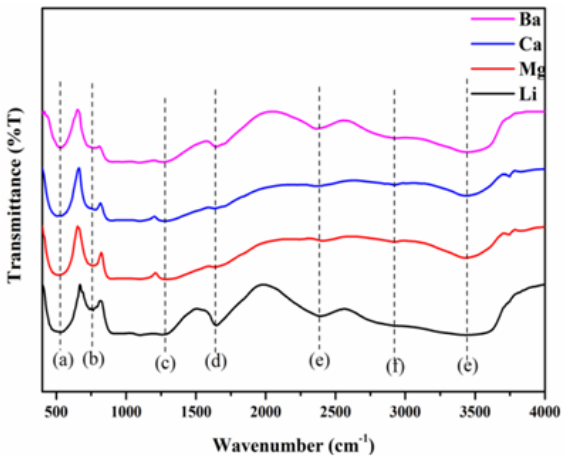

FIG.3

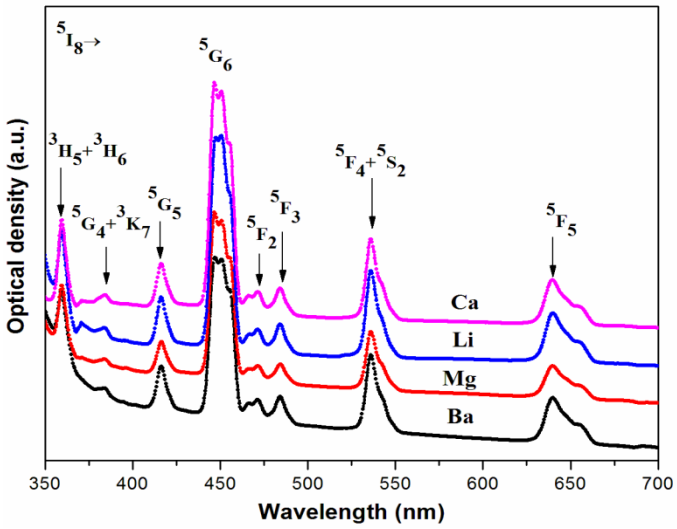

FIG.4

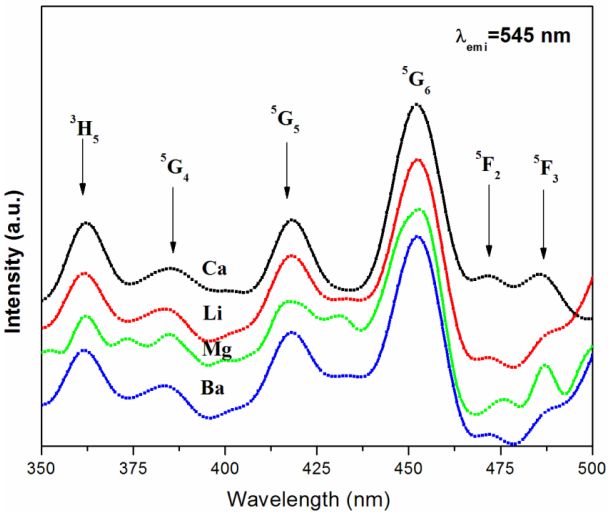

Fig. 5

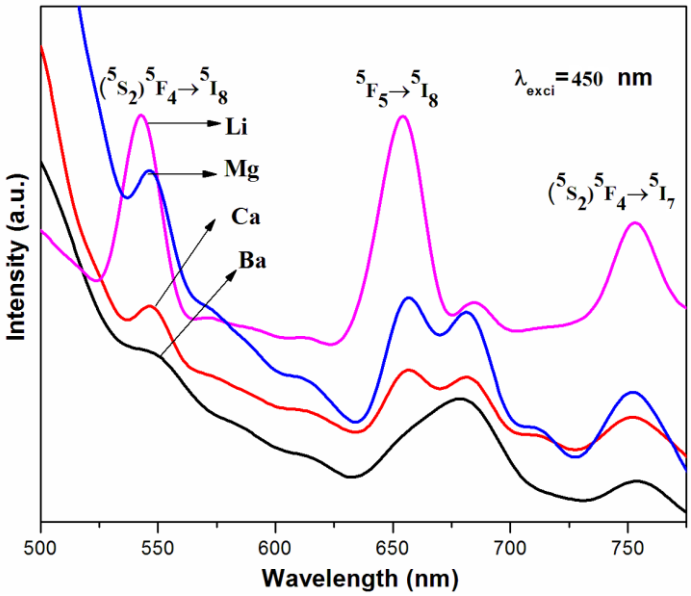

Fig. 6

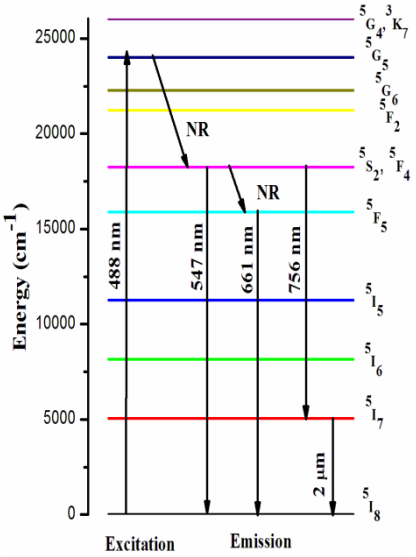

Fig. 7

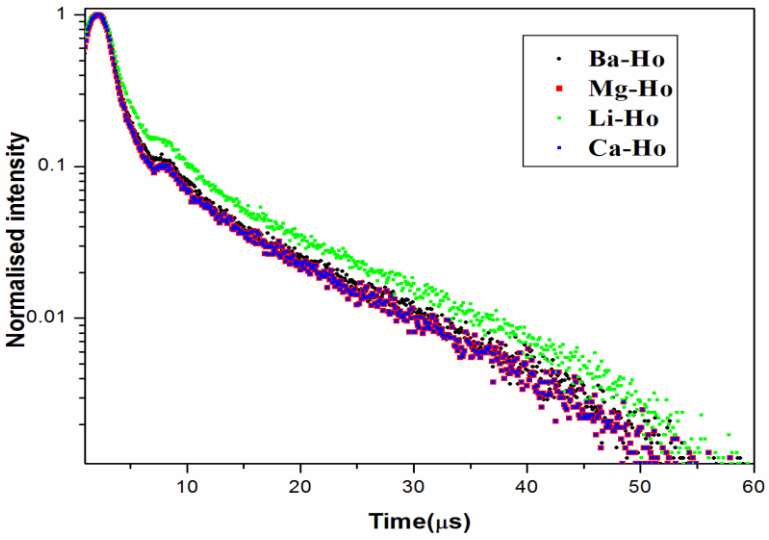

Fig. 8

Table 1 Experimental ($f_{exp}x10^{-6}$) and calculated ($f_{cal}x10^{-6}$) spectral intensities of observed absorption bands of Ho^{3+} doped different phosphate glasses.

Absorption band	Li		Mg		Ca		Ba	
	f_{exp}	f_{cal}	f_{exp}	f_{cal}	f_{exp}	f_{cal}	f_{exp}	f_{cal}
$^3H_5+^3H_6$	8.12	8.67	8.13	8.22	8.02	7.81	5.16	5.34
$^3G_4+^3K_7$	1.39	1.47	1.49	1.40	1.15	1.39	0.64	0.98
$^5G_5$	7.65	7.93	6.56	6.92	7.34	7.17	4.96	4.91
$^5G_6$	43.16	42.89	40.92	40.75	38.99	37.79	26.34	26.52
$^5F_2$	0.93	1.74	0.827	1.78	1.44	1.74	1.30	1.26
$^5F_3$	2.33	2.86	2.61	2.93	2.35	2.86	1.42	2.07
$^5F_4+^5S_2$	9.88	9.70	9.83	9.51	9.90	9.43	6.88	6.73
$^5F_5$	8.07	7.72	7.59	7.28	7.08	7.33	4.85	5.16
δ_{rms}	±0.56		±0.53		±0.67		±0.38	

Table 2 Comparison of J-O parameters (Ω_λ $x10^{-20}$ cm^2) and spectroscopic quality factors (χ) of Ho^{3+} doped different host compositions

Glass Matrix	Ω_2	Ω_4	Ω_6	(χ)	References
Li	5.65	3.76	2.38	0.63	Present work
Mg	5.33	3.41	2.54	0.74	Present work
Ca	4.82	3.48	2.44	0.70	Present work
Ba	3.32	2.40	1.78	0.74	Present work
Oxy fluoride tellurite	4.20	2.80	1.10	0.39	[30]
$LuSiO_3$ Crystal	4.57	3.11	1.42	0.45	[31]
Gallium Lanthanum Sulphide	6.90	5.50	1.07	0.19	[32]
Oxy fluoride(Si based)	5.84	2.38	1.75	0.73	[33]

Table 3 Energies ($\Delta\nu$, cm^{-1}), electric dipole line strengths ($s_{ed}x10^{20}$ $/e^2$ cm^2), radiative transition probabilities (A_{ed}, s^{-1}), radiative branching ratios (β_R) and integrated absorption cross sections ($\sum x10^{18}$) for different excited states of Ho^{3+} doped lithium phosphate glass.

Transition	$\Delta\nu$	S_{ed}	A_{ed}	β_R	$\sum$
$^3H_5\rightarrow{}^3K_7$	1731	120.17	1.7	0	0.28
$^5G_4$	1980	79.4	1.7	0	0.21
$^5G_5$	3767	67.56	9.7	0	0.33
$^5F_1$	5629	15.82	7.6	0.001	0.12
$^5G_6$	5503	64.6	28.8	0	0.46
$^3K_8$	6449	7.01	5	0.001	0.06
$^5F_2$	6478	46.65	34	0.004	0.39
$^5F_3$	7151	100.17	98.2	0.015	0.94
$^5F_4$	9123	169.38	344.6	0.002	2.02
$^5S_2$	9370	21.57	47.6	0.003	0.26
$^5F_5$	12190	124.99	606.7	0.002	1.99
$^5I_4$	15552	5.54	55.8	0.016	0.11
$^5I_5$	16581	30.36	370.9	0.125	0.66
$^5I_6$	19081	152.97	2847.8	0.62	3.81
$^5I_7$	22664	453.49	14147.2	0.185	13.42
$^5I_8$	27800	73.25	4217.3	0	2.66
$^5G_6\rightarrow{}^3K_8$	946	75.01	0.1	0	0.05
$^5F_2$	975	32.5	0.1	0	0.05
$^5F_3$	1648	60.95	0.6	0.001	0.11
$^5F_4$	3620	252.78	27.2	0	1.1
$^5S_2$	3867	118.73	15.6	0.015	0.51
$^5F_5$	6687	737.11	499.8	0	5.45
$^5I_4$	10049	0.75	1.7	0.002	0.01
$^5I_5$	11078	23.66	72.9	0.011	0.29
$^5I_6$	13578	61.61	349.7	0.106	0.92
$^5I_7$	17161	301.5	3455.4	0.864	5.72
$^5I_8$	22297	1120.25	28160	0	27.61
$^3K_8\rightarrow{}^5F_2$	29	0.86	0	0	0
$^5F_3$	702	1.59	0	0	0
$^5F_4$	2674	3.36	0.1	0	0.01
$^5S_2$	2921	0	0	0.004	0
$^5F_5$	5741	14.22	4.7	0.002	0.07
$^5I_4$	9103	2.02	2.6	0.002	0.02
$^5I_5$	10132	1.13	2	0.025	0.01
$^5I_6$	12632	8.02	28	0.08	0.09
$^5I_7$	16215	12.17	90	0.887	0.17
$^5I_8$	21351	59.21	999.4	0.887	1.07

$^5F_2 \rightarrow {}^5F_3$	673	27.35	0	0.001	0
$^5F_4$	2645	42.28	4.6	0	0.32
$^5S_2$	2832	2.16	0.3	0.008	0.02
$^5F_5$	5712	36.85	40.5	0.069	0.61
$^5I_4$	9074	82.85	365	0.104	2.16
$^5I_5$	10103	89.76	545.8	0.201	2.61
$^5I_6$	12603	89.5	1056.4	0.089	3.24
$^5I_7$	16186	18.78	469.5	0.528	0.87
$^5I_8$	21322	48.58	2776.5	0	2.98
$^5F_3 \rightarrow {}^5F_4$	1972	85.28	2.8	0	0.35
$^5S_2$	2219	3.31	0.2	0.006	0.02
$^5F_5$	5039	71.73	38.7	0.049	0.74
$^5I_4$	8401	131.01	327.1	0.046	2.26
$^5I_5$	9403	85.76	302.9	0.092	1.66
$^5I_6$	11930	85.27	609.8	0.347	2.09
$^5I_7$	15513	145.25	2308.9	0.46	4.68
$^5I_8$	20649	82.44	3056.8	0	3.49
$^5F_4 \rightarrow {}^5S_2$	247	6.76	0	0.002	0
$^5F_5$	3067	140.32	13.3	0.009	0.69
$^5I_4$	6429	70.5	61.4	0.032	0.72
$^5I_5$	7458	161.93	22.0	0.064	1.93
$^5I_6$	9958	137.7	445.4	0.096	2.19
$^5I_7$	13541	81.62	663.8	0.797	1.76
$^5I_8$	13677	258.28	5511.6	0	7.7
$^5F_5 \rightarrow {}^5I_4$	3362	3.2	0.3	0	0.01
$^5I_5$	4391	53.09	12	0.003	0.3
$^5I_6$	6891	170.97	149.9	0.039	1.54
$^5I_7$	10474	236.9	729.5	0.188	3.24
$^5I_8$	15610	293.64	2993.1	0.77	5.99

Table 4 Radiative properties (A_T in s^{-1}), (τ_R in µs) for certain excited states of Ho^{3+} doped different phosphate glass matrices

Glass	$^3H_5$		$^5G_6$		$^3K_8$		$^5F_2$		$^5F_3$		$^5F_4$	
	A_T	τ_R	A_T	τ_R	A_T	τ_R	A_T	τ_R	A_T	τ_R	A_T	τ_R
Li	22824	44	32588	31	1126	888	5258	190	6647	150	6916	145
Mg	22837	44	32421	31	1168	856	5498	182	6826	146	6984	143
Ca	21550	46	30480	33	1122	891	5339	187	6671	150	6868	146
Ba	14948	67	21033	48	802	1247	3848	250	4779	209	4892	203

Table 5 Emission band positions (λ_p (nm)), effective band widths ($\Delta\nu_{eff}$), transition probabilities (A_R) and experimental branching ratios (β_R), radiative life times (τ_R) (µs) and peak stimulated emission cross section ($\sigma_{e*10}{}^{-20}$ cm^2) for observed emission transitions of Ho^{3+} doped different phosphate glasses.

Transition	Parameters	Li	Mg	Ca	Ba
$(^5S_2)\,{}^5F_4 \rightarrow {}^5I_8$	λ_p	543.3	547.8	547.1	547.2
	A_R	5511	5632	5515	3944
	$\Delta\nu_{eff}$	329.7	153.0	44.37	36.5
	β_{exp}	0.180	0.182	0.203	0.148
	τ_R	1.44	1.43	1.45	2.04
	σ_e	8.09	7.45	6.57	6.72
$^5F_5 \rightarrow {}^5I_8$	λ_p	653.9	657.1	682.5	681.3
	A_R	2993	2966	2931	2078
	$\Delta\nu_{eff}$	490.3	395.8	416.0	373
	β_{exp}	0.576	0.574	0.584	0.673
	τ_R	2.57	2.79	2.92	3.70
	σ_e	1.44	1.91	1.88	1.50
$(^5S_2)\,{}^5F_4 \rightarrow {}^5I_7$	λ_p	752.8	763	752.1	757.8
	A_R	664	618	626	434
	$\Delta\nu_{eff}$	261.4	146.8	226.2	165
	β_{exp}	0.244	0.234	0.261	0.200
	τ_R	1.44	1.43	1.45	2.04
	σ_e	0.79	1.49	0.89	0.87

Table 6 Branching ratios (β_R) and integrated absorption cross-sections ($\sum$) (10^{-18} sec) of certain transitions of Ho^{3+} doped different phosphate glass matrices.

Glass	$^3H_5 \rightarrow {}^5I_7$		$^5G_6 \rightarrow {}^5I_7$		$^3K_8 \rightarrow {}^5I_7$		$^5F_2 \rightarrow {}^5I_7$		$^5F_3 \rightarrow {}^5I_7$		$^5F_4 \rightarrow {}^5I_7$		$^5F_5 \rightarrow {}^5I_8$	
	β_R	$\sum$	β_R	$\sum$	β_R	$\sum$	β_R	$\sum$	β_R	$\sum$	β_R	$\sum$	β_R	$\sum$
Li	0.185	13.42	0.864	5.72	0.887	0.17	0.528	0.87	0.46	4.68	0.797	1.76	0.77	5.99
Mg	0.185	2.65	0.866	27.46	0.886	1.10	0.544	3.21	0.483	3.76	0.806	7.85	0.769	5.92
Ca	0.193	2.62	0.862	25.69	0.886	1.06	0.538	3.08	0.475	3.61	0.803	7.69	0.769	5.84
Ba	0.198	1.86	0.86	17.76	0.886	0.76	0.544	2.24	0.482	2.63	0.806	5.52	0.77	4.15

Table 7 Measured (τ_{mes} μs) and calculated (τ_{cal} μs) radiative lifetimes and quantum efficiencies (η,%) of $^5F_5$ state of Ho^{3+} in different phosphate glasses.

Glass	τ_{mes}	τ_{cal}	η
Li	2.06	2.57	80
Mg	2.15	2.79	77
Ca	2.12	2.92	72
Ba	2.42	3.70	65

IV. CONCLUSION

In the present work, Ho^{3+} doped different phosphate glasses are prepared by melt quenching technique and characterized through different structural and spectroscopic measurements. XRD and SEM images confirmed the non-crystalline nature of the prepared phosphate glass. On the basis of ^{31}P MAS NMR analysis, a decrease in the proportion of Q^2 units in the sequence Li-Ca-Ba-Mg in these different component host glasses are observed which indicates that these oxides were incorporated into the glass as network modifier oxides. From the absorption spectra, spectral intensities, J-O intensity parameters (Ω_2, Ω_4 and Ω_6), radiative transition probabilities (A_T), radiative lifetimes (τ_R) and branching ratios (β_R) are obtained for different phosphate glasses doped with Ho^{3+} ion. Among the three J-O parameters, Ω_2 has higher for Li phosphate glass which indicated higher covalency of ligand field. Ω_6 parameter has higher in Mg phosphate glass and lower in Ba phosphate glass indicating higher and lower rigidies and viscosities. From the emission spectra, peak stimulated emission cross-sections (σ_e) are calculated for the observed emission transitions in four different phosphate glasses doped with Ho^{3+} ion. Among all the glasses, Li glass matrix showed higher stimulated emission cross-section for $^5S_2(^5F_4) \rightarrow {}^5I_8$ transition. From the emission spectra, experimental branching ratios are also reported. From the fluorescence decay profiles, it is observed that decay curves exhibit non-exponential behavior for all glass matrices. Hence, Li phosphate glass doped with Ho^{3+} ion can be suitable to produce efficient red laser emission.

Acknowledgements

The authors acknowledge MOU-DAE-BRNS project (No.2009/34/36/BRNS/3174), Department of Physics, S .V .University, Tirupati India for extending experimental facility.

REFERENCES

[1]. A.A. Kaminski, L.K. Aminov, V.L. Ermolev, E.B. Sveshni kova, I. Fizika , 1986 (in Russia).
[2]. B. Henderson, R.H. Bartram, Crystal -field of Engineering of Soild State Lasers Materials, 2000.
[3]. H.T. Yuen, J.C. Daniel, A.K. Terence, Opt. Commun., 231, 2004, 357.
[4]. Y.J. Zhang, Y.Z. Wang, Y.L. Ju, B.Q. Yao, Laser Opto electronics progress, 42, 2005, 34.
[5]. G. J. Koch, M. Petros, J. Yu, U.N. Singh, Appl. Opt. 41, 2002, 1718.
[6]. K. Scholle, E. Heumann, G. Huber, Laser Phys. Lett.1, 2004, 285.
[7]. T. J. Suratwal , R.A . Steela, G. D. Wike , J. K. Campbell, K. Takenchi, J. Non-Cryst. Solids 263, 2000, 213.
[8]. B. Suresh, Ya. Zhydachevski, M.G. Brik , A. Suchocki, M. Sreenivas Reddy,
[9]. Piasecki, N. Veeraiah , J. Alloy Compd., 683, 2016, 114.Z. Xing, S. Gao, X . Liu, S. Sun, C. Yu, L. Xiung, K. Li, M. Liao, J. Alloy. Compd., 660,2016, 375.
[10]. N. Rakov, G.S. Maciel, C.B. de Araujo, J. Appl. Phys. 91, 2002, 1272.
[11]. S.B. Rai, Spectrochim. Acta A 58, 2002, 1559.
[12]. Ch. Srinivasa Rao, K .Upendra Kumar, P. Babu, C.K. Jayasankar, Opt. Mater., 35, 2012,102
[13]. X. Liu, P. Kuan, D. Li, S. Gao, X. Wang, L. Zhang, L.Hu, D. Chen, Opt. Mater. Express 6, 2016, 1093.
[14]. B. Peng, T. Izumitani, Opt. Mater., 4, 1995, 701.
[15]. M. Seshadri, Y.C. Ratnakaram, D. Tirupathi Naidu, K. Venkata Rao, Opt. Mater. 32, 2010, 535.
[16]. C.R. Kesavulu, H.J. Kim, S.W. Lee, J. Kaewkhaeo, N. Wantana, S. Kothan, S. Kaewjaeng J.Non - Cryst. Solids, 2017.
[17]. Rong Chen, Ying Tian, Bingpeng Li, Fengchao Wang, Xufeng Jing , Junjie Zhang, Shiqing Xu Opt. Mat., 49, 2015, 116.
[18]. Ch. Srinivasa Rao, K. Upendra Kumar, P. Babu, C.K. Jayasankar, Opt. Mat., 35, 2015, 102.
[19]. V. Ravi Kumar, G. Giridhar, V. Sudarsan, N. Veeraiah J. Alloys and compd., 695,2017, 668.
[20]. Ying Tian, Liyan Zhang, Suya Feng, Rongrong Xu, Lili Hu, Junjie Zhang Opt. Mat. 32, 2010, 1508.
[21]. A. Marzouk, F.H. ElBatal, A.M. Abdelghany, Spectchim. Acta Part A, 114, 2013, 658.
[22]. Meiqing Shi, Yanjie Lian, Liyuan Chai, Xiaobo Min,Zongwen Zhao, Shu Yang, J. Mol. Struct., 1081, 2015, 389.
[23]. Mingwei Lu, Fu Wang, Qilong Liao, Kuiru Chen, JianfaQin, Sheqi Pan, J. Mol. Struct., 1081,2015, 187.

[24]. C.K. Jayasankar, E. Rukimini, Physica B 240, 1997, 273.
[25]. W.T. Carnall, G.L. Good man, K. Rajnak, R.S. Rana, J. Chem. Phys. 90, 1989, 3443.
[26]. B. R. Judd. Phys. Rev., 127, 1962, 750.
[27]. G .S .Ofelt, J. Chem, Phys., 37, 1962, 511.
[28]. M. Ajroud, M. Haouari, H. Ben Quada, H. Maaref, A. Brenier, C. Garapon, J. Phys. : Condens. Mat., 12, 2000, 318.
[29]. K. Kadono, T.Yazawa, M. Shojiya, K. Kawomoto, J. Non-Cryst. Soilds. 274, 2000, 75.
[30]. G. Gao, G. Wanga, C. Yu, J. Zhang, L. Hu, J. Lumin., 129, 2009, 1042.
[31]. Q. Dong, G. Zhao, J. Chen, Y. Ding, B. Yao, Z. Yu, Opt. Mater., 32, 2010, 873.
[32]. T. Schweizer, B. N. Samson, J.R. Hector, W. S. Brockiesby, D.W. Hewak, D.N. Payne Infrared Phys. Technol., 40, 1999, 329.
[33]. L. Feng, J. Wang, Q. Tang, L.F. Liang, H.B Liang, Q. Su. J. Lumin., 124, 2007, 187.
[34]. G.V. Prakash, Mater. Lett., 46, 2000, 15.
[35]. A.cMajjane, A. Chahine, M. Et - tabirou, B. Echchahed, Trong-on Do, P. M. C. Breen Mater.Chem. Phys., 143, 2014, 779.
[36]. M. Shojiya, M. Takashi, R. Kanno, J. Appl. Phys., 82, 1997, 6259.
[37]. Huilong Guo, Jifu Bi,Jiayi wang, Xuequan zhang, Shichun Jiang, Zhonghua wu, Dalton Trans, 44, 2015, 9130.

B. Haritha "Spectral Investigations And Emission Properties Of Ho3+ Doped Different Phosphate Glasses For 2µm Laser Materials "International Journal of Engineering Science Invention (IJESI), vol. 07, no. 05, 2018, pp 07-17